IEEE Access
Multidisciplinary ⋮ Rapid Review ⋮ Open Access Journal

Received September 28, 2020, accepted October 9, 2020, date of publication October 13, 2020, date of current version October 26, 2020.

Digital Object Identifier 10.1109/ACCESS.2020.3030805

Robust Adaptive Finite-Time Tracking Control for Uncertain Euler-Lagrange Systems With Input Saturation

CHAO CHEN[1], GUIBING ZHU[1], QAING ZHANG[2], AND JIANWEI ZHANG[1]
[1]Maritime College, Zhejiang Ocean University, Zhoushan 316022, China
[2]Navigation College, Shandong Jiaotong University, Weihai 264209, China

Corresponding author: Guibing Zhu (master2186980@sohu.com)

This work was supported in part by the National Natural Science Foundation of China under Grant 51809237, and in part by the Key Research and Development Plan of Shandong Province under Grant 2019JZZY020712.

ABSTRACT In this paper, a robust adaptive finite-time (FT) tracking control scheme is proposed for Euler-Lagrange systems (ELSs) subject to nonparametric uncertainties, unknown disturbances and input saturation. In the design procedure, a Gaussian error function is utilized to approximate the input saturation nonlinearity. Following that, by employing the natural property that the upper bound of model parameters uncertainties is linear-in-parameters, the lumped uncertain term caused by uncertain model parameters and external disturbances is formulated by a linear-parametric form with a single parameter. And then, a novel robust adaptive tracking control law is designed to resolve the tracking control problem of uncertain ELSs. The proposed control scheme is featured by FT convergence rate, and robustness against uncertainties and unknown disturbances. Furthermore, the robust adaptive FT tracking control scheme is insensitive to the character of the uncertainties, and is with low computational burden and easy to implement in engineering applications. And its rigorous stability is analyzed with the aid of the Lyapunov stability theory, and its effectiveness is verified by simulation results and comparison.

INDEX TERMS Euler-Lagrange systems, finite time, uncertainty, robust adaptive control, input saturation.

I. INTRODUCTION

It is well known that Euler-Lagrange systems (ELSs) can describe the motion behaviors of a wide number of physical systems, including robotic manipulators [1], [2], aircrafts [3], surface ships [4], underwater vehicles [5], etc. In parctice, the uncertainties are frequently encountered in the operations of ELSs due to unmodeled nonlinearities, unknown parameters and external disturbances, which make the tracking control problem challenging. To solve these issues and improve the tracking control performance of ELSs, many control schemes have been presented, such as intelligent control [6]–[8], adaptive control [9]–[11], robust control [12], [13], and sliding mode control (SMC) [14], [15]. Intelligent control schemes and adaptive control schemes are the powerful tools for the uncertain ELSs, whereas the online computation issue becomes the biggest obstacle to these schemes [16], [17]. Compared with intelligent control schemes and adaptive control schemes, robust control schemes and SMC schemes can reduce the computation complexity. Nevertheless, they require the predefined bound of the uncertainties, and the SMC suffers from the so-called chattering problem [18]. More recently, adaptive robust control (ARC) [19], [20] and adaptive SMC [21]–[23] were proposed for the uncertain systems described by ELSs, which were neither computationally intensive nor required the predefined bound. Although these control schemes have extraordinary advantage in theory and applications, all of them are merely ensured by uniform or asymptotic stability, which implies the system trajectory converges to the equilibrium states in infinite time. In order to achieve fast convergence, an effective approach is to greatly increase the control gain. In practice, however, the high gain control is undesirable and would be unimplemented. Consequently, it is essential for uncertain ELSs to develop a control scheme featured by fast convergence and strong robustness.

Recently, the finite-time (FT) control has attracted interesting attention from many scholars [24], [25]. Compared with

The associate editor coordinating the review of this manuscript and approving it for publication was Shuping He.

the uniform or asymptotic stability, FT stability may give rise to better transient and steady-state performance and can make the system trajectory converge to an equilibrium point in finite time. Inspired by these attributes, a FT regulation control scheme [26] and a global continuous FT tacking control scheme [27] were respectively proposed for the robot manipulators. However, both of the schemes require that the model knowledge be accurately known. For the tracking control problem of ELSs with model perturbations, terminal sliding-mode control (TSMC) [28], [29], non-singular terminal sliding-mode control (NTSMC) [30] and passivity-based SMC [31] were proposed to achieve the FT stable control. Regarding the TSMC/NTSMC scheme, the system states can reach a non-linear finite-time convergent sliding mode, namely, TSM in a finite time, then converge to the equilibrium along the TSM in a finite time. Nevertheless, a common assumption in [28]–[31] was that the unknown parts must be obeyed to one function of sliding variable or system states, where the function must be known. Even if these control schemes [28]–[31] avoided the inherent chattering in SMC [14], [15]. However, in practice, it is not always possible to obtain such a *prior* knowledge. To circumvent the limit, the adaptive technique and neural network (NN) technique were incorporated into TSMC [32], [33] and NTSMC [34]–[38] design to achieve the FT tracking control of robotic manipulators. In [32] and [35], the normal parts of plants are required; in [34], the uncertainties need to satisfy parameterized decomposition conditions and the acceleration of ELSs is required to be available. Although [32] and [36] discard the assumption mentioned in [33]–[35], the computational complexity problem still exists. In addition, the schemes above-mentioned neglect an issue, i.e., any real systems are subjected to the inherent physical limit of actuator (the input saturation nonlinearity).

In general, the effect of input saturation would be disastrous due to the nonlinearities and uncertainties of the plants [37]. Hence, when the input saturation is neglected in the control design, the proposed control schemes may be fail their goal. For uncertain ELSs under input saturation, [38] proposed an adaptive tracking control scheme, where the saturated linear correction term was designed to comply with the imposed input saturation; [39] developed a robust adaptive model reference impedance control scheme, where an auxiliary dynamic system (ADS) was constructed for compensating the effect of input saturation. However, in [38], [39], the uncertainties must satisfy the parameterized decomposition conditions. Using the same ADS as [39], [40] developed an adaptive neural impedance control scheme. Note that the schemes developed in [38]–[40] can not ensure the FT stability of system. To do that, a FT tracking control solution was presented for robot manipulators with actuator saturation by Proportional-Differential plus dynamics compensation method [41], whereas the system dynamics were required to be accurately known. For the tracking control problem of rigid spacecraft subject to model parameter perturbations and input saturation, the non-singular fast terminal sliding mode control (FTNFTSMC) was employed to solve the control problem since it is of the feature of overcoming input singularity [42], where a modified ADS was designed to handle the input saturation effect. Obviously, the control scheme can not directly be transplanted to solve the tracking control problem of the uncertain ELSs with input saturation. Thus, further researches on robust tracking control mechanism for uncertain ELSs with input saturation to ensure the FT convergence capability of closed-loop system is being expected.

Motivated by the above-mentioned discussion, this paper aims to solve the tracking control problem for uncertain ELSs with input saturation. Firstly, a Gaussian error function is used to approximate the input saturation nonlinearities. Then, according to the structural properties of ELSs that the upper bounds of uncertain model parameters are linear-in-parameters (LIP) [19], [31], and utilizing the LIP structure, the lumped uncertainty including nonparametric uncertainties, unknown disturbances and approximate error is transformed into a linear parametric form with a single parameter instead of being assumed to upper bounded by a known function or constant. Finally, a novel robust adaptive tracking control scheme is developed for achieving FT tracking control of uncertain ELSs. The main contributions of this work include:

- The proposed control scheme achieves FT tracking of ELSs in the simultaneous presence of nonparametric uncertainties, unknown disturbances and input saturation.
- Unlike [9]–[11], [22], [23] and [34], where the uncertainties need to satisfy parameterized decomposition conditions, the uncertainties in our work are formulated by a linear parametric form with a single parameter such that the proposed scheme is insensitive to the character of the uncertainties.
- Compared with [33]–[36], [40], [42], any *prior* knowledge regarding of uncertain model parameters and disturbances in this work are not needed and only one unknown parameter in this work needs to be updated online. Hence, the proposed scheme is featured by low computational burden and easy to implement in engineering applications.

The remainder of this work is organized as follows. Section 2 states the formulated problem and some preliminaries. Section 3 gives the main results, and the simulation results are presented in Section 4, including comparisons. Section 5 draws the conclusions.

Notations: In this paper, R^+ denotes the set of nonnegative real numbers and R denotes the set of real numbers. For a given matrix or vector $\boldsymbol{Y}$, $\|\boldsymbol{Y}\|$ represents the 2-norm of $\boldsymbol{Y}$. For any a scalar $m \in R$ and vector $\boldsymbol{\rho} \in R^n$, $\rho^m = \left[\rho_1^m, \cdots, \rho_n^m\right]^T$. $\lambda_{max}(\cdot)$ and $\lambda_{min}(\cdot)$ denote the maximum and minimum eigenvalues of a matrix, respectively. sgn $(\cdot)$ represent the sign function. $\boldsymbol{I_n}$ denotes a n-dimensional identity matrix.

II. PROBLEM FORMULATION

In general, the EL systems with the second-order dynamics can be described as follows:

$$\boldsymbol{H}(\boldsymbol{q})\ddot{\boldsymbol{q}}+\boldsymbol{C}(\boldsymbol{q},\dot{\boldsymbol{q}})+\boldsymbol{G}(\boldsymbol{q})+\boldsymbol{F}(\boldsymbol{q},\dot{\boldsymbol{q}})=\boldsymbol{\tau}+\boldsymbol{d} \tag{1}$$

where $\boldsymbol{q}\in R^n$ denotes the system state, $\boldsymbol{\tau}=[\tau_1,\cdots,\tau_n]^T$ is the control input, and $\boldsymbol{d}\in R^n$ denotes the external disturbance vector.$\boldsymbol{H}(\boldsymbol{q})$, $\boldsymbol{C}(\boldsymbol{q},\dot{\boldsymbol{q}})$, $\boldsymbol{G}(\boldsymbol{q})$ and $\boldsymbol{F}(\boldsymbol{q},\dot{\boldsymbol{q}})$ denote the mass/inertial matrix, the matrix of Coriolis and centripetal matrix, the gravity matrix, and the friction matrix, respectively.

In practice, due to the physical constraints of the actuator, the input saturation nonlinearity can be expressed by

$$\tau_i=\begin{cases}\operatorname{sgn}\left(\tau_{i,c}\right)\tau_{i,m}, & \text{if } \tau_{i,c}>\tau_{i,m}\\ \tau_{i,c}, & \text{if } \tau_{i,c}\le\tau_{i,m}\end{cases}\quad i=1,\cdots,n \tag{2}$$

where $\tau_{i,c}$ denotes the command control of ith actuator calculated by the control law and $\tau_{i,m}>0$ denotes represents the maximum control input provided by the ith actuator.

In system (1), $\boldsymbol{H}(\boldsymbol{q})$, $\boldsymbol{C}(\boldsymbol{q},\dot{\boldsymbol{q}})$, $\boldsymbol{G}(\boldsymbol{q})$ and $\boldsymbol{F}(\boldsymbol{q},\dot{\boldsymbol{q}})$ possess the following properties [19], [31]:

Property 1: $\boldsymbol{H}(\boldsymbol{q})$ is symmetric and positive definite matrix and there exist two unknown constants $\hbar$ and h that satisfy $\hbar\boldsymbol{I_n}\le\boldsymbol{H}(\boldsymbol{q})\le h\boldsymbol{I_n}$.

Property 2: $\exists C_d\in R^+$,such that $\|\boldsymbol{C}(\boldsymbol{q},\dot{\boldsymbol{q}})\|\le C_d\|\dot{\boldsymbol{q}}\|$.

Property 3: $\exists F_d, G_d\in R^+$,such that $\|\boldsymbol{F}(\boldsymbol{q},\dot{\boldsymbol{q}})\|\le F_d\|\dot{\boldsymbol{q}}\|$ and $\|\boldsymbol{G}(\boldsymbol{q})\|\le G_d$.

To facilitate the control design, we make the following standard assumptions:

Assumption 1: $\boldsymbol{d}$ is bounded and there exists an unknown constant $\bar{d}$ that satisfies $\|\boldsymbol{d}\|\le\bar{d}$.

*Assumption 2:*The desired trajectory $\boldsymbol{q_d}\in R^n$, and its first and second order derivatives are bounded and available.

The control objective of this paper is to design a robust adaptive tracking control law $\boldsymbol{\tau_c}$ for the uncertain ELS (1) subject to input saturation under Assumptions 1-2 such that the output $\boldsymbol{q}$ of the system (1) tracks a desired trajectory $\boldsymbol{q_d}$, and the tracking error converges to a small neighborhood in finite time, while ensuring that all signals in closed-loop tracking system are bounded.

It is clearly from (2) that the relationship between the actual control input $\boldsymbol{\tau}$ and the designed control input $\boldsymbol{\tau_c}$ has a sharp corner when $|\tau_{i,c}|=\tau_{i,m}, i=1,\cdots,n$. According to [43], the saturation nonlinearity function defined in (2) can be approximated by the following smooth function

$$\xi_i(\tau_{i,c})=\tau_{i,m}\mathcal{E}\left(\frac{\sqrt{\pi}\tau_{i,c}}{2\tau_{i,m}}\right) \tag{3}$$

where $\mathcal{E}(\cdot)$ is a Gaussian error function, which is defined as $\mathcal{E}(x)=\frac{2}{\sqrt{\pi}}\int_0^x e^{-t^2}\,dt$. From (2)-(3), $d_{i,\tau}=\tau_i-\xi_i(\tau_{i,c})$, where $|d_{i,\tau}|\le\bar{d}_{i,\tau}$ with $\bar{d}_{i,\tau}$ being a constant. Using the mean-value theorem, $\xi_i(\tau_{i,c})$ can be expressed as

$$\xi_i(\tau_{i,c})=\xi_i(0)+\vartheta_i\tau_{i,c} \tag{4}$$

where $\vartheta_i=e^{-\left(\frac{\sqrt{\pi}\iota\tau_{i,c}}{2\tau_{i,\max}}\right)^2}$ and $\iota\in(0,1)$. Thus, we have

$$\tau_i=\vartheta_i\tau_{i,c}+d_i\left(\tau_{i,c}\right) \tag{5}$$

Remark 1: According to the definition of ϑ_i, we know that ϑ_i is bounded. That is, for $\forall\tau_{i,c}\in R$, there exist positive constants $\vartheta_{i,1}$ and $\vartheta_{i,2}$ such that $0<\vartheta_{i,1}\le\vartheta_i\le\vartheta_{i,2}$. In addition, due to $\left|d_{i,\tau}\right|\le\bar{d}_{i,\tau}$, we obtain $\|\boldsymbol{d_\tau}\|=\left\|\left[d_{i,\tau},\cdots,d_{n,\tau}\right]\right\|\le\bar{d}_\tau$ with $\bar{d}_\tau>0$ being unknown constant.

Synthesizing (1) and (5), we have

$$\boldsymbol{H}(\boldsymbol{q})\ddot{\boldsymbol{q}}+\boldsymbol{C}(\boldsymbol{q},\dot{\boldsymbol{q}})+\boldsymbol{F}(\boldsymbol{q},\dot{\boldsymbol{q}})=\boldsymbol{\vartheta}\boldsymbol{\tau}_c+\boldsymbol{d_\Delta} \tag{6}$$

where $\boldsymbol{\vartheta}=diag\left(\vartheta_1\cdots\vartheta_n\right)$ and $\boldsymbol{d_\Delta}=\boldsymbol{d}+\boldsymbol{d_\tau}$. According to Assumption 1 and $\|\boldsymbol{d_\tau}\|\le\bar{d}_\tau$, d_Δ is bounded. That is, there exists a unknown constant $d_s>0$ satisfying $\|\boldsymbol{d_\Delta}\|\le d_s$.

For the later control design purpose, the following lemmas are stated.

Lemma 1 [44]: For real numbers x and y, and any constants $a>0$, $b>0$ and $\ell>0$, the following inequality holds.

$$|x|^a|y|^b\le\frac{a}{a+b}\ell|x|^{a+b}+\frac{b}{a+b}\ell^{-\frac{a}{b}}|y|^{a+b} \tag{7}$$

Lemma 2 [29]: For any real numbers a_i, $i=1,\cdots,n$ and any $r\in(0,1)$, the following inequality holds

$$\left(\sum_{i=1}^{n}|a_i|\right)^r\le\sum_{i=1}^{n}|a_i|^r \tag{8}$$

Lemma 3 [29]: For any scalars $c_1>0, c_2>0$ and $\nu\in(0,1)$, an extended Lyapunov condition of finite-time stability can be given as $\dot{V}(x)+c_1V(x)+c_2V^\nu(x)\le0$,where the setting time is given by $T\le\frac{1}{c_1(1-\nu)}\ln\frac{c_1V^{1-\nu}(x_0)+c_2}{c_2}$ with the initial value $V(x_0)$.

III. MAIN RESULTS

In this section, we will investigate the robust adaptive FT control scheme for the tracking control problem of ELSs in the simultaneous presence of nonparametric uncertainties, unknown disturbances and input saturation. In the control design, utilizing the Properties 1-3, the lumped uncertainties including uncertain model parameters, $\boldsymbol{d}$ and $\boldsymbol{d}_\tau$ are formulated by a linear parametric form with a single parameter. Then, a robust adaptive FT control law is designed for the uncertain ELSs.

Define the tracking error vector $\boldsymbol{e}_1=\boldsymbol{q}-\boldsymbol{q}_d$. Further, we have $\boldsymbol{e_2}=\dot{\boldsymbol{e_1}}=\dot{\boldsymbol{q}}-\dot{\boldsymbol{q_d}}$. Here, the following polynomial on $\boldsymbol{e_1}$ and $\boldsymbol{e_2}$ is designed

$$\boldsymbol{S}=\boldsymbol{e_2}+\boldsymbol{\alpha}\boldsymbol{e_1}+\boldsymbol{\beta}\boldsymbol{\psi}(\boldsymbol{e_1}) \tag{9}$$

where $\boldsymbol{\alpha}=diag\left(\alpha_1,\cdots,\alpha_n\right)$ and $\boldsymbol{\beta}=diag\left(\beta_1,\cdots,\beta_n\right)$ with α_i and β_i being positive scalars, and $\boldsymbol{\psi}(\boldsymbol{e_1})=\left[\psi\left(e_{1,1}\right),\cdots,\psi\left(e_{1,n}\right)\right]^T$ with

$$\psi\left(e_{1,i}\right)=\begin{cases}e_{1,i}^{\lambda} & \left|e_{1,i}\right|>\zeta\\ l_1e_{1,i}+l_2e_{1,i}^2\operatorname{sgn}\left(e_{1,i}\right) & \left|e_{1,i}\right|\le\zeta\end{cases} \tag{10}$$

Here, $l_1 = (2-\lambda)\zeta_i^{\lambda-1}$ and $l_2 = (2-\lambda)\zeta_i^{\lambda-2}$ with $\zeta \in (0,1)$ being a small constant. $0 < \lambda = \lambda_1/\lambda_2 < 1$ is design constant, and λ_1 and λ_2 are positive odd integers.

Lemma 4: Consider the system (6) and (9), if $\boldsymbol{S}$ can be guaranteed to converge to a domain in a finite time, $\boldsymbol{e_1}$ and $\boldsymbol{e_2}$ can converge to a small region around origin in finite-time T_e.

Proof: Choose the Lyapunov function as $V_e = 0.5\boldsymbol{e}_1^T\boldsymbol{e}_1$. Taking the derivative of V_e yields $\dot{V}_e = \boldsymbol{e}_1^T\boldsymbol{e}_2$.

Using (9), $\dot{V}_e$ is given by

$$\dot{V}_e = -\gamma_{\min}(\boldsymbol{\alpha})\,\boldsymbol{e_1}^T\boldsymbol{e_1} - \boldsymbol{e_1}^T\boldsymbol{\beta}\boldsymbol{\psi}(\boldsymbol{e_1}) + \boldsymbol{e_1}^T\boldsymbol{S} \tag{11}$$

Here, let

$$\digamma_i(e_{1,i}) = e_{1,i}^{\lambda+1} - l_1 e^2{}_{1,i} - l_2\left|e_{1,i}\right|^3, \quad i = 1,\cdots,n \tag{12}$$

In the light of (10), $\digamma_i(e_{1,i})$ is bounded when $\left|e_{1,i}\right| \le \zeta$, i.e., $\sum_{i=1}^{n}\left|\digamma_i(e_{1,i})\right| \le \bar{\zeta}$ and $\bar{\zeta} > 0$. Thus,

$$\begin{cases} -\boldsymbol{e}_1^T\boldsymbol{\psi}(\boldsymbol{e}_1) = \sum_{i=1}^{n} e_i^{\lambda+1} & \left|e_{1,i}\right| > \zeta \\ -\boldsymbol{e}_1^T\boldsymbol{\psi}(\boldsymbol{e}_1) \le -\sum_{i=1}^{n} e_i^{\lambda+1} + \sum_{i=1}^{n}\left|\digamma_i(e_{1,i})\right| & \left|e_{1,i}\right| \le \bar{\zeta} \end{cases} \tag{13}$$

According to (13), one can get

$$-\boldsymbol{e}_1^T\boldsymbol{\psi}(\boldsymbol{e}_1) \le -\sum_{i=1}^{n} e_i^{\lambda+1} + \bar{\zeta} \tag{14}$$

Using (14), (11) can be rewritten as

$$\begin{aligned} \dot{V}_e \le& -(\gamma_{\min}(\boldsymbol{\alpha}) - 1)\,\boldsymbol{e_1}^T\boldsymbol{e_1} - \gamma_{\min}(\boldsymbol{\beta})\left(\sum_{i=1}^{n} e_{1,i}^2\right)^{\frac{\lambda+1}{2}} \\ &+ \frac{||\boldsymbol{S}||^2}{4} + \gamma_{\min}(\boldsymbol{\beta})\,\bar{\zeta} \\ \le& -2(\gamma_{\min}(\boldsymbol{\alpha}) - 1)\,V_e - \gamma_{\min}(\boldsymbol{\beta})\,2^{\frac{\lambda+1}{2}}V_e^{\frac{\lambda+1}{2}} \\ &+ \frac{||\boldsymbol{S}||^2}{4} + \gamma_{\min}(\boldsymbol{\beta})\,\bar{\zeta} \end{aligned} \tag{15}$$

From (15), due to the boundedness of $\boldsymbol{S}$, it can be obtained that $\boldsymbol{e_1}$ and $\boldsymbol{e_2}$ are bounded. If $V_e \ge \frac{||\boldsymbol{S}||^2 + 4\gamma_{\min}(\boldsymbol{\beta})\bar{\zeta}}{8(\gamma_{\min}(\boldsymbol{\alpha}) - 1)\varsigma}$ with ς being a positive scalar, it can be obtained

$$\dot{V}_e \le -2(1-\varsigma)(\gamma_{\min}(\boldsymbol{\alpha}) - 1)\,V_e - \gamma_{\min}(\boldsymbol{\beta})\,2^{\frac{\lambda+1}{2}}V_e^{\frac{\lambda+1}{2}} \tag{16}$$

According to Lemma 3 and (16), V_e converges to a neighbourhood in a finite time, i.e., $\boldsymbol{e_1}$ also converges to a neighbourhood $\Omega_e = \left\{\boldsymbol{e_1} \mid ||\boldsymbol{e_1}|| \le \sqrt{\frac{||\boldsymbol{S}||^2 + 4\gamma_{\min}(\boldsymbol{\beta})\bar{\zeta}}{4(\gamma_{\min}(\boldsymbol{\alpha}) - 1)\varsigma}}\right\}$ in a finite time, and the time T_e can be estimated as

$$T_e \le \frac{\ln\left(\frac{2(1-\varsigma)(\gamma_{\min}(\boldsymbol{\alpha})-1)V^{\frac{1-\lambda}{2}}(0) + \gamma_{min}(\boldsymbol{\beta})2^{\frac{\lambda+1}{2}}}{\gamma_{min}(\boldsymbol{\beta})2^{\frac{\lambda+1}{2}}}\right)}{(1-\varsigma)(\gamma_{\min}(\boldsymbol{\alpha}) - 1)(1-\lambda)} \tag{17}$$

where $V_e(0)$ is the initial value of V_e. Recalling (9) and (16), if $\boldsymbol{S}$ can be guaranteed to converge to a domain in a finite time, both $\boldsymbol{e_1}$ and $\boldsymbol{e_2}$ converge to a small neighbourhood. Thus, the Lemma 4 is proved.

Let $\boldsymbol{\Lambda} = \boldsymbol{\alpha}^{-1}\boldsymbol{\beta}$ and $\boldsymbol{E}(\boldsymbol{e}) = \boldsymbol{\Lambda}\boldsymbol{\psi}(\boldsymbol{e}_1) + \boldsymbol{e}_1$. From (9), $\boldsymbol{S}$ can be written as

$$\boldsymbol{S} = \boldsymbol{\Xi}\left[\boldsymbol{E}^T(\boldsymbol{e}_1)\ \boldsymbol{e}_2^T\right]^T \tag{18}$$

where $\boldsymbol{\Xi} = [\boldsymbol{\beta} \quad \boldsymbol{I_n}]$. Using (10), we have $\|\boldsymbol{e}_2\| \le \|\boldsymbol{\Xi}^{-1}\|\|\boldsymbol{S}\|$. Due to $\boldsymbol{e}_2 = \dot{\boldsymbol{q}} - \dot{\boldsymbol{q}}_d$, then $\|\dot{\boldsymbol{q}}\| \le \|\boldsymbol{\Xi}^{-1}\|\|\boldsymbol{S}\| + \|\dot{\boldsymbol{q}}_d\|$. Further, according to Properties 2-3, we have

$$\|\boldsymbol{C}(\boldsymbol{q},\dot{\boldsymbol{q}})\| \le C_d\|\boldsymbol{\Xi}^{-1}\|\|\boldsymbol{S}\| + C_d\|\dot{\boldsymbol{q}}_d\| \tag{19}$$

$$\|\boldsymbol{F}(\boldsymbol{q},\dot{\boldsymbol{q}})\| \le F_d\|\boldsymbol{\Xi}^{-1}\|\|\boldsymbol{S}\| + F_d\|\dot{\boldsymbol{q}}_d\| \tag{20}$$

Taking the derivative of $\boldsymbol{S}$ along (9), and using (6) and $\boldsymbol{e}_2 = \dot{\boldsymbol{q}} - \dot{\boldsymbol{q}}_d$, it can be get

$$\begin{aligned} \dot{\boldsymbol{S}} &= \ddot{\boldsymbol{q}} - \ddot{\boldsymbol{q}}_d + (\boldsymbol{\alpha} + \boldsymbol{\beta}\boldsymbol{\psi_f}(\boldsymbol{e}_1))\,\boldsymbol{e}_1 \\ &= \boldsymbol{H^{-1}}(\boldsymbol{q})\Big[\boldsymbol{\vartheta}\boldsymbol{\tau_c} + \boldsymbol{d}_\triangle - \boldsymbol{C}(\boldsymbol{q},\dot{\boldsymbol{q}}) - \boldsymbol{G}(\boldsymbol{q}) \\ &\quad - \boldsymbol{H}(\boldsymbol{q})\ddot{\boldsymbol{q}}_d + \boldsymbol{H}(\boldsymbol{q})\left(\boldsymbol{\alpha} + \boldsymbol{\beta}\boldsymbol{\psi}_f(\boldsymbol{e}_1)\right)\boldsymbol{e}_2\Big] \end{aligned} \tag{21}$$

where $\boldsymbol{\psi}_f(\boldsymbol{e}_1) = \left[\psi_f(e_{1,1}),\cdots,\psi_f(e_{1,n})\right]^T$ and $\psi_f(e_{1,i}) = \begin{cases} \lambda e_i^{\lambda-1} & \left|e_{1,i}\right| > \zeta \\ l_1 + 2l_2\left|e_{1,i}\right| & \left|e_{1,i}\right| \le \zeta \end{cases}$.

Here, let

$$\begin{aligned} \boldsymbol{\phi} = \boldsymbol{d}_\triangle - \boldsymbol{C}(\boldsymbol{q},\dot{\boldsymbol{q}})\dot{\boldsymbol{q}} - \boldsymbol{G}(\boldsymbol{q}) - \boldsymbol{F}(\boldsymbol{q},\dot{\boldsymbol{q}}) - \boldsymbol{H}(\boldsymbol{q})\ddot{\boldsymbol{q}}_d \\ + \boldsymbol{H}(\boldsymbol{q})(\boldsymbol{\alpha} + \boldsymbol{\beta}\boldsymbol{\psi}_f(\boldsymbol{e}_1))\boldsymbol{e}_2 \end{aligned} \tag{22}$$

Using Property 1, $\|\boldsymbol{d}_\triangle\| \le d_s$ and (19)-(20), one can obtain

$$\begin{aligned} \|\boldsymbol{\phi}\| \le& d_s + C_d\left(\left\|\boldsymbol{\Xi}^{-1}\right\|\|\boldsymbol{S}\| + \left\|\dot{\boldsymbol{q}}_d\right\|\right)^2 + G_d F_d\left\|\boldsymbol{\Xi}^{-1}\right\|\|\boldsymbol{S}\| \\ &+ F_d\left\|\dot{\boldsymbol{q}}_d\right\| + h\left\|\ddot{\boldsymbol{q}}_d\right\| + h\left\|\boldsymbol{\Xi}^{-1}\right\|\Big(||\boldsymbol{\alpha}|| \\ &+ ||\boldsymbol{\beta}||\left\|\boldsymbol{\psi}_f(\boldsymbol{e}_1)\right\|\Big)\|\boldsymbol{S}\| \\ \le& C_d\left\|\boldsymbol{\Xi}^{-2}\right\|\|\boldsymbol{S}\|^2 + \Big(2C_d\left\|\boldsymbol{\Xi}^{-1}\right\|\left\|\dot{\boldsymbol{q}}_d\right\| + F_d\left\|\boldsymbol{\Xi}^{-1}\right\| \\ &+ h\left\|\boldsymbol{\Xi}^{-1}\right\|||\boldsymbol{\alpha}||\Big)\|\boldsymbol{S}\| + h||\boldsymbol{\beta}||\left\|\boldsymbol{\psi}_f(\boldsymbol{e}_1)\right\|\|\boldsymbol{S}\| \\ &+ h\left\|\ddot{\boldsymbol{q}}_d\right\| + \left\|\dot{\boldsymbol{q}}_d\right\|^2 + f_b\left\|\dot{\boldsymbol{q}}_d\right\| + d_s + G_d \end{aligned} \tag{23}$$

Since $\dot{\boldsymbol{q}}_d$ and $\ddot{\boldsymbol{q}}$ are bounded, it can be verified using (14) that $\exists\delta \in R^+$, such that the upper bound of $\boldsymbol{\phi}$ holds the following form:

$$\|\boldsymbol{\phi}\| \le \delta\left[\|\boldsymbol{S}\|^2 + (\|\boldsymbol{\psi}_f(\boldsymbol{e}_1)\| + 1)\|\boldsymbol{S}\| + 1\right] = \delta(\boldsymbol{S}) \tag{24}$$

where $\delta = \max\Big\{C_d, 2C_d\left\|\boldsymbol{\Xi}^{-1}\right\|\left\|\dot{\boldsymbol{q}}_d\right\| + F_d\left\|\boldsymbol{\Xi}^{-1}\right\| + h\left\|\boldsymbol{\Xi}^{-1}\right\|||\boldsymbol{\alpha}||, h||\boldsymbol{\beta}||, h\left\|\ddot{\boldsymbol{q}}_d\right\| + \left\|\dot{\boldsymbol{q}}_d\right\|^2 + F_d\left\|\dot{\boldsymbol{q}}_d\right\| + d_s + G_d\Big\}$ and $\varrho(\boldsymbol{S}) = \|\boldsymbol{S}\|^2 + \left(\left\|\boldsymbol{\psi}_f(\boldsymbol{e}_1)\right\| + 1\right)\|\boldsymbol{S}\| + 1$.

Remark 2: In practice, system uncertainties frequently encountered must be coped with in ELSs controller design to guarantee desired performance. This issue is not resolved with well in the study of [28]–[31]. Therefore the control law developed in [28]–[31] cannot be applied to deal with non-parametric uncertainties. In this context, employing the LIP structure of ELSs, the lumped uncertain term $\boldsymbol{\phi}$ is transformed into a linear parametric form as shown in (20).

Remark 3: In [7], [33], [40], the NNs and fuzzy logic systems are applied to approximate the unknown term $\boldsymbol{\mathcal{B}} = \boldsymbol{H}(\boldsymbol{q})\ddot{\boldsymbol{q}}_d + \boldsymbol{C}(\boldsymbol{q},\dot{\boldsymbol{q}})\dot{\boldsymbol{q}}_d + \boldsymbol{G}(\boldsymbol{q}) + \boldsymbol{F}(\boldsymbol{q},\dot{\boldsymbol{q}}) - \boldsymbol{d}$. In [9]–[11] and [23], the parameterized decomposition condition is required, that is, $\boldsymbol{H}(\boldsymbol{q})\ddot{\boldsymbol{q}}_d + \boldsymbol{C}(\boldsymbol{q},\dot{\boldsymbol{q}})\dot{\boldsymbol{q}}_d + \boldsymbol{G}(\boldsymbol{q}) + \boldsymbol{F}(\boldsymbol{q},\dot{\boldsymbol{q}}) = \boldsymbol{Y}\left(\boldsymbol{q},\dot{\boldsymbol{q}},q_d,\dot{\boldsymbol{q}}_d\right)\Theta$, where $\boldsymbol{Y}\left(\boldsymbol{q},\dot{\boldsymbol{q}},\boldsymbol{q}_d,\dot{\boldsymbol{q}}_d\right) \in R^{n\times n}$ is known regression matrix and $\boldsymbol{\Theta} \in R^n$ is unknown constant vector. In those literature, obviously, a large number of parameters need to be online estimated. As a result, the computation complexity problem is unavoidable. In [19], $\|\boldsymbol{\phi}\| \leq a_0 + a_1\|\boldsymbol{\xi}\| + a_2\|\boldsymbol{\xi}\|^2 = \boldsymbol{Y}^T(\boldsymbol{\xi})\boldsymbol{\epsilon}$, where $\boldsymbol{\xi} = [\boldsymbol{e}_1,\boldsymbol{e}_2]^T$, $\boldsymbol{Y}(\boldsymbol{\xi}) = \left[1, \|\boldsymbol{\xi}\|, \|\boldsymbol{\xi}\|^2\right]^T$ and $\boldsymbol{\epsilon} = [a_0,a_1,a_2]^T$. Here, only three parameters need to be online estimated, which can overcome the computation complexity problem. From (24), only one parameter in this work need to be online estimated. Therefore, the proposed scheme is simple to compute and easy to implement in engineering applications.

Remark 4: It should be noted that an implicit assumption in [7], [33], [40] is that the variable $\boldsymbol{q}$ and $\boldsymbol{q}_d$ are presupposed to be bounded. It is quite clear that such an assumption is conservative since the bounds of $\boldsymbol{q}$ and $\boldsymbol{q}_d$ are unknown. As a result, it is difficult to guarantee the reconstruction accuracy of the unknown term $\boldsymbol{\mathcal{B}}$ because the boundary of the domain of basis function is difficult to determine. Fortunately, in this work, such an implicit assumption is deserted by using the LIP structure of ELSs. As a result, this challenging problem is easily avoided.

Using (23), (20) can be further written as

$$\begin{aligned}\boldsymbol{S}^T\dot{\boldsymbol{S}} &\leq \boldsymbol{S}^T\boldsymbol{H}^{-1}(q)\boldsymbol{\vartheta}\boldsymbol{\tau}_c + \left\|\boldsymbol{S}^T\boldsymbol{H}^{-1}(\boldsymbol{q})\boldsymbol{\phi}\right\| \\ &\leq \boldsymbol{S}^T\boldsymbol{H}^{-1}(q)\boldsymbol{\vartheta}\boldsymbol{\tau}_c + \theta\varrho(\boldsymbol{S})\,||\boldsymbol{S}|| \end{aligned} \tag{25}$$

where $\theta = h\delta$. Since $\boldsymbol{M}(\boldsymbol{q})$ and $\boldsymbol{\vartheta}$ are positive-definite matrixes.

To achieve the control objective, the following control law is designed

$$\boldsymbol{\tau}_c = -\boldsymbol{k}_1\boldsymbol{S} - \boldsymbol{k}_2\boldsymbol{S}^\lambda - \kappa\hat{\theta}\varrho^2(\boldsymbol{S})\boldsymbol{S} \tag{26}$$

with the adaptive laws

$$\dot{\hat{\theta}} = \kappa\varrho^2(\boldsymbol{S})\|\boldsymbol{S}\|^2 - \sigma\hat{\theta}, \quad \hat{\theta}(0) \geq 0 \tag{27}$$

where $\boldsymbol{k}_i = \boldsymbol{k}_i^T \in R^{n\times n}$, $i = 1,2$, are positive-definite design matrixes. $\kappa > 0$ and $\sigma > 0$ are design constants.

Remark 5: From (9), (23) and (24), the term $\varrho(s)$ is a function of the variable $\boldsymbol{S}$, which indicates that the designed control law $\boldsymbol{\tau}_c$ only needs the first-derivative of the desired trajectory $\boldsymbol{q}_d$, i.e., this work only requires that $\dot{\boldsymbol{q}}_d$ be available. In contrast, it indicates that the condition on $\boldsymbol{q}_d$ is less stringent in our work.

Consider the following Lyapunov function

$$V = \frac{1}{2}\boldsymbol{S}^T\boldsymbol{S} + \frac{1}{2\chi}\left(\theta - \chi\hat{\theta}\right)^2 \tag{28}$$

Taking the time derivative of V and using (21), (25)-(27) yield

$$\begin{aligned}\dot{V} &\leq \boldsymbol{S}^T\left[\boldsymbol{H}^{-1}(\boldsymbol{q})\boldsymbol{\vartheta}\boldsymbol{\tau}_c + \boldsymbol{\phi}\right] - \left(\theta - \chi\hat{\theta}\right)\dot{\hat{\theta}} \\ &\leq -\boldsymbol{S}^T\boldsymbol{H}^{-1}(\boldsymbol{q})\boldsymbol{\vartheta}\boldsymbol{k}_1\boldsymbol{S} - \boldsymbol{S}^T\boldsymbol{H}^{-1}(\boldsymbol{q})\boldsymbol{\vartheta}\boldsymbol{k}_2\boldsymbol{S}^\lambda \\ &\quad -\kappa\hat{\theta}\varrho^2(\boldsymbol{S})S^T\boldsymbol{H}^{-1}(\boldsymbol{q})\boldsymbol{\vartheta}\boldsymbol{S} + \|\boldsymbol{S}\|\theta\varrho(\boldsymbol{S}) \\ &\quad -\left(\theta - \chi\hat{\theta}\right)\kappa\varrho^2(\boldsymbol{S})\|\boldsymbol{S}\|^2 + \sigma\left(\theta - \chi\hat{\theta}\right)\hat{\theta} \end{aligned} \tag{29}$$

Using Young's inequality, the following inequations hold

$$\|\boldsymbol{S}\|\theta\varrho(\boldsymbol{S}) \leq \kappa\theta\varrho^2(\boldsymbol{S})\|\boldsymbol{S}\|^2 + \frac{\theta}{4\kappa} \tag{30}$$

$$\begin{aligned}\left(\theta - \chi\hat{\theta}\right)\hat{\theta} &= \frac{1}{\chi}\left(\theta - \chi\hat{\theta}\right)\left(\chi\hat{\theta} - \theta + \theta\right) \\ &\leq -\frac{1}{2\chi}\left(\theta - \chi\hat{\theta}\right)^2 + \frac{1}{2\chi}\theta^2 \end{aligned} \tag{31}$$

From the Property 1 and Remark 1, there exists a positive constant χ such that $\chi \leq \lambda_{\min}\left(\boldsymbol{H}^{-1}(\boldsymbol{q})\boldsymbol{\vartheta}\right)$ holds. Then, the following inequations hold

$$\chi\boldsymbol{S}^T\boldsymbol{S} \leq \boldsymbol{S}^T\boldsymbol{H}^{-1}(\boldsymbol{q})\boldsymbol{\vartheta}\boldsymbol{S} \tag{32}$$

$$\chi\boldsymbol{S}^T\boldsymbol{S}^\lambda \leq \boldsymbol{S}^T\boldsymbol{H}^{-1}(\boldsymbol{q})\boldsymbol{\vartheta}\boldsymbol{S}^\lambda \tag{33}$$

Substituting (23)-(24) and (30)-(33) into (29) yields

$$\begin{aligned}\dot{V} &\leq -\chi\gamma_{\min}(\boldsymbol{k}_1)\boldsymbol{S}^T\boldsymbol{S} - \chi\gamma_{\min}(\boldsymbol{k}_2)\boldsymbol{S}^T\boldsymbol{S}^\lambda \\ &\quad -\kappa\chi\hat{\theta}\varrho^2(\boldsymbol{S})\boldsymbol{S}^T\boldsymbol{S} + \kappa\theta\varrho^2(\boldsymbol{S})\|\boldsymbol{S}\|^2 \\ &\quad -\left(\theta - \chi\hat{\theta}\right)\kappa\varrho^2(\boldsymbol{S})\|\boldsymbol{S}\|^2 + \frac{\theta}{4\kappa} \\ &\quad -\frac{\sigma}{2\chi}\left(\theta - \chi\hat{\theta}\right)^2 + \frac{\sigma}{2\chi}\theta^2 \\ &= -\chi\gamma_{\min}(\boldsymbol{k}_1)S^TS - \chi\gamma_{\min}(\boldsymbol{k}_2)\boldsymbol{S}^T\boldsymbol{S}^\lambda \\ &\quad -\frac{\sigma}{2\chi}\left(\theta - \chi\hat{\theta}\right)^2 - \left[\frac{\sigma}{4\chi}\left(\theta - \chi\hat{\theta}\right)^2\right]^{\frac{\lambda+1}{2}} \\ &\quad +\left[\frac{\sigma}{4\chi}\left(\theta - \chi\hat{\theta}\right)^2\right]^{\frac{\lambda+1}{2}} + \frac{\theta}{4\kappa} + \frac{\sigma}{2\chi}\theta^2 \end{aligned} \tag{34}$$

Here, let $x = 1$, $y = \frac{\sigma}{4\chi}\left(\theta - \chi\hat{\theta}\right)^2$, $a = \frac{1-\lambda}{2}$, $b = \frac{1+\lambda}{2}$ and $\ell = \left(\frac{1+\lambda}{2}\right)^{\frac{1+\lambda}{1-\lambda}}$. Then, $a + b = 1$, $\frac{a}{a+b} = a$ and $\frac{b}{a+b} = b$. Further, we have $\frac{a}{a+b}\ell|x|^{a+b} + \frac{b}{a+b}\ell^{-\frac{a}{b}}|y|^{a+b} = \frac{1-\lambda}{2}\ell + \frac{\sigma}{4\chi}\left(\theta - \chi\hat{\theta}\right)^2$ and $|x|^a|y|^b = \left[\frac{\sigma}{4\chi}\left(\theta - \chi\hat{\theta}\right)^2\right]^{\frac{1+\lambda}{2}}$. According to Lemma 1, one can get

$$\left[\frac{\sigma}{4\chi}\left(\theta - \chi\hat{\theta}\right)^2\right]^{\frac{\lambda+1}{2}} \leq \frac{1-\lambda}{2}\ell + \frac{\sigma}{4\chi}\left(\theta - \chi\hat{\theta}\right)^2 \tag{35}$$

Using (35), (34) can be written as

$$\begin{aligned}\dot{V} &\leq -\chi\gamma_{\min}(\boldsymbol{k}_1)\boldsymbol{S}^T\boldsymbol{S} - \chi\gamma_{\min}(\boldsymbol{k}_2)\boldsymbol{S}^T\boldsymbol{S}^\lambda \\ &\quad -\frac{\sigma}{4\chi}\left(\theta - \chi\hat{\theta}\right)^2 - \left[\frac{\sigma}{4\chi}\left(\theta - \chi\hat{\theta}\right)^2\right]^{\frac{\lambda+1}{2}} \\ &\quad +\frac{1-\lambda}{2}\ell + \frac{\theta}{4\kappa} + \frac{\sigma}{2\chi}\theta^2 \end{aligned} \tag{36}$$

In the light of Lemma 2, the following inequality holds

$$
\begin{aligned}
&-\chi\gamma_{\min}(\boldsymbol{k}_2)\boldsymbol{S}^T\boldsymbol{S}^{\lambda}-\left[\frac{\sigma}{4\chi}\left(\theta-\chi\hat{\theta}\right)^2\right]^{\frac{\lambda+1}{2}}\\
&\quad=-\chi\gamma_{\min}(\boldsymbol{k}_2)\sum_i^n\left(S_i^2\right)^{\frac{\lambda+1}{2}}-\left[\frac{\sigma}{4\chi}\left(\theta-\chi\hat{\theta}\right)^2\right]^{\frac{\lambda+1}{2}}\\
&\quad\le-2^{\frac{\lambda+1}{2}}\chi\gamma_{\min}(\boldsymbol{k}_2)\left(0.5\sum_i^n s_i^2\right)^{\frac{\lambda+1}{2}}\\
&\qquad-\left(\frac{\sigma}{2}\right)^{\frac{\lambda+1}{2}}\left[\frac{1}{2\chi}\left(\theta-\chi\hat{\theta}\right)^2\right]^{\frac{\lambda+1}{2}}\\
&\quad\le-\mu V^{\frac{\lambda+1}{2}}
\end{aligned}
\tag{37}
$$

where $\mu=\min\left\{-2^{\frac{\lambda+1}{2}}\chi\gamma_{\min}(\boldsymbol{k}_2),\left(\frac{\sigma}{2}\right)^{\frac{\lambda+1}{2}}\right\}$.

Substituting (37) into (36) yields

$$
\begin{aligned}
\dot{V}&\le-\chi\gamma_{\min}(k_1)S^TS-\frac{\sigma}{4\chi}\left(\theta-\chi\hat{\theta}\right)^2\\
&\quad-\mu V^{\frac{\lambda+1}{2}}+\frac{1-\lambda}{2}\ell+\frac{\theta}{4\kappa}+\frac{\sigma}{2\chi}\\
&\le-\mu_0V-\mu V^{\frac{\lambda+1}{2}}+C
\end{aligned}
\tag{38}
$$

where $\mu_0 = \min\left\{\chi\gamma_{\min}(\boldsymbol{k}_1),\frac{\sigma}{2}\right\}$ and $C=\frac{1-\lambda 2}{\ell}+\frac{\theta}{4\kappa}+\frac{\sigma}{2\chi}\theta^2$.

Based on the above design and analysis, there is the following theorem.

Theorem 1: Consider the ELS given in (1) in the simultaneous presence of nonparametric uncertainties, unknown disturbances and input saturation under Assumptions 1-2. The proposed robust adaptive finite-time control law (26) with adaptive law (27) can ensure the following statements:

1) The sliding mode variable S in finite-time converges into the following region

$$\|\boldsymbol{S}\|\le\sqrt{\frac{2C}{\ell\mu_0}}\tag{39}$$

where ℓ is a positive constant satisfying $\ell\in(0,1)$.

2) The tracking error e_1 in finite-time converges into the following region

$$\|\boldsymbol{e}_1\|\le\sqrt{\frac{C+2\gamma_{\min}(\boldsymbol{\beta})\bar{\varsigma}\ell\mu_0}{2\ell\mu_0(\gamma_{\min}(\boldsymbol{\alpha})-1)\varsigma}}\tag{40}$$

3) All the signals in closed-loop tracking control system are bounded.

Proof: From (38), $\dot{V}\le-\mu_0V+C$ holds and solving it yields

$$0\le V(t)\le\frac{C}{\mu_0}+\left[V(0)-\frac{C}{\mu_0}\right]e^{-\mu_0t}\tag{41}$$

where $V(0)$ is the initial value of V. Therefore, $V(t)$ is bounded. It follows from (28) that $\boldsymbol{S}$ and $\theta-\chi\hat{\theta}$ are bounded. Furthermore, $\hat{\theta}$ is bounded due to the boundedess of θ, and the tracking error e_1 and its derivative e_2 are bounded owing to the Lemma 4 and the boundedness of S. Thus, $\varphi(\boldsymbol{e}_1,\boldsymbol{S})$ is also bounded. Following that, the designed control law $\boldsymbol{\tau_c}$ in (26)) is also bounded. Therefore, the all the signals in closed-loop tracking control system are bounded.

Recalling (38), we have

$$\dot{V}\le-\ell\mu_0V-(1-\ell)\mu_0V-\mu_1V^{\frac{\lambda+1}{2}}+C\tag{42}$$

If $V\ge\frac{C}{\ell\mu_0}$, we have

$$\dot{V}\le-(1-\ell)\mu_0V-\mu_1V^{\frac{\lambda+1}{2}}\tag{43}$$

According to Lemma 3, V in finite time settles within the set $\Omega_V=\left\{V|V\le\frac{C}{\ell\mu_0}\right\}$ and the settling time is given by

$$T\le\frac{1}{(1-\ell)\mu_0}\ln\frac{(1-\ell)\mu_0V^{\frac{1-\lambda}{2}}(0)+\mu_1}{\mu_1}\tag{44}$$

In addition, from (28), $\frac{1}{2}\boldsymbol{S}^T\boldsymbol{S}\le V\le\frac{C}{\ell\mu_0}$ holds. $\|\boldsymbol{S}\|\le\varpi=\sqrt{\frac{2C}{\ell\mu_0}}$. Furthermore, in view of Lemma 4, the trajectory of the closed-loop tracking control system converges to a small region in finite time. Obviously, we can not directly obtain the region of the tracking error e_1 from $\|\boldsymbol{S}\|\le\varpi$. According to Lemma 4 and $\|\boldsymbol{S}\|\le\varpi$, the following formula can be obtained

$$\|\boldsymbol{e}_1\|\le\sqrt{\frac{C+2\gamma_{\min}(\boldsymbol{\beta})\bar{\varsigma}\ell\mu_0}{2\ell\mu_0(\gamma_{\min}(\boldsymbol{\alpha})-1)\varsigma}}\tag{45}$$

Thus, Theorem 1 is proved.

IV. SIMULATION

To verify the effectiveness of the proposed FT tracking control scheme, the two-link robotic manipulator (RM) is considered. The dynamics of the RM [31] are given by (1) with

$$\boldsymbol{H}(\boldsymbol{q})=\begin{bmatrix}\Omega_1+2\Omega_2\cos(q_2) & \Omega_3+\Omega_2\cos(q_2)\\ \Omega_3+\Omega_2\cos(q_2) & \Omega_3\end{bmatrix}\tag{46}$$

$$\boldsymbol{C}(\boldsymbol{q},\dot{\boldsymbol{q}})=\begin{bmatrix}-\Omega_2\dot{q}_2\sin(q_2) & -\Omega_2(\dot{q}_1+\dot{q}_2)\sin(q_2)\\ \Omega_2\dot{q}_1\sin(q_2) & 0\end{bmatrix}\tag{47}$$

$$\boldsymbol{G}(\boldsymbol{q})=\begin{bmatrix}\Omega_4 g\cos(q_1)+\Omega_5 g\cos(q_1+q_2)\\ \Omega_5\cos(q_1+q_2)\end{bmatrix}\tag{48}$$

$$\boldsymbol{F}(\boldsymbol{q},\dot{\boldsymbol{q}})=\begin{bmatrix}\Omega_6\tanh(\dot{q}_1)\\ \Omega_6\tanh(q_2)\cos(q_1+q_2)\end{bmatrix}\tag{49}$$

$$\boldsymbol{d}=\begin{bmatrix}0.25\cos(0.1\pi t)\sin(0.5t)\\ 0.125\sin(0.15t)\sin(t/4)\cos(0.02t)\end{bmatrix}\tag{50}$$

where $\boldsymbol{q}=[q_1,q_2]^T$, $\Omega_1=m_1l_1^2+m_2L_1^2+m_2l_2^2+\Gamma_2+\Pi_1$, $\Gamma_2=m_2L_1l_2$, $\Omega_3=+m_2l_2^2+\Pi_2$, $\Omega_4=m_1l_2+m_2L_1$, $\Omega_5=m_2l_1$, and $\Omega_6=0.5.m_i$, $i=1,2$, is the mass of the ith link with $m_1=1.6$kg and $m_2=0.8$kg; L_i is the length of the ith link with $L_1=0.4\ m$; l_i is the distance from the base of the ith link to its center of mass with $l_1=0.25m$ and $l_2=0.15m$; Γ_i is the inertia moment of the ith link with $\Gamma_1=0.0853kg\cdot m^2$ and $\Gamma_2=0.024kg\cdot m^2$ and $g=9.81m/s$ is the gravitation constant.

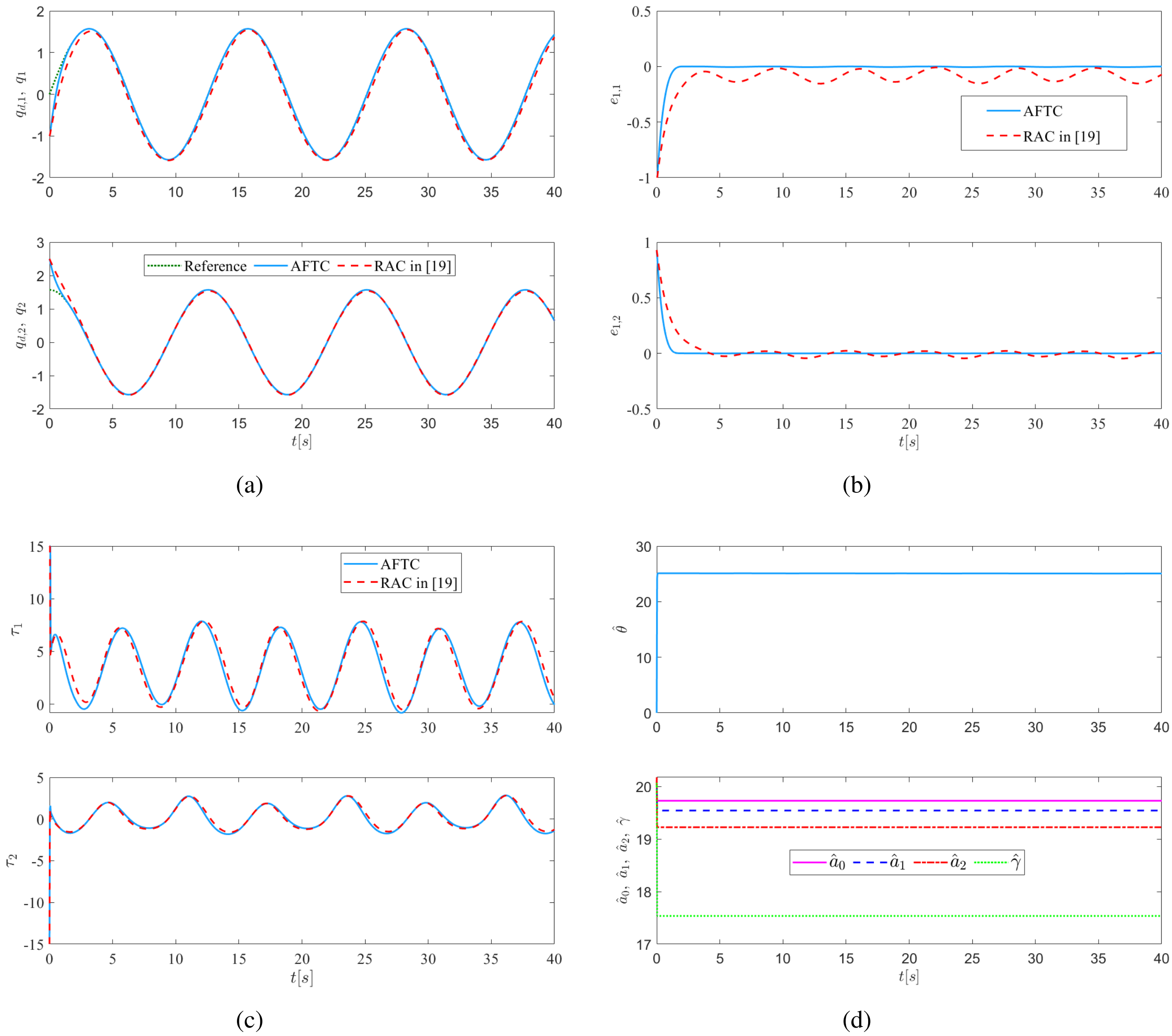

FIGURE 1. Simulation results under AFTC and ARC. (a) Tracking performance. (b) Tracking error e_1. (c) Control input τ. (d) Estimation of θ and a_i, $i = 0, 1, 2$.

A. EFFECTIVENESS TEST

In the simulation, the desired trajectory is set as $\boldsymbol{q}_d = 0.5\pi\,[\sin(0.5t), \cos(0.5t)]^T\,(rad)$. The saturation limit is given by $\tau_{i,m} = 15\,(N \cdot m)\,, i = 1, 2$. The initial states are $\boldsymbol{q}(0) = [-1rad, 2.5rad]^T$, $\dot{\boldsymbol{q}}(0) = [0, 0]^T$ and $\hat{\theta}_i(0) = 0$. The design parameters are selected as $\boldsymbol{\alpha} = diag(2, 2)$, $\boldsymbol{\beta} = diag(1, 1)$, $\boldsymbol{k}_1 = diag(8, 8)$, $\boldsymbol{k}_2 = diag(10, 10)$, $\kappa = 1$, $\zeta = 0.001$, $\sigma = 0.0001$, and $\lambda = \frac{3}{5}$.

The simulation results under the proposed adaptive FT control (AFTC) scheme are plotted using solid line in Fig. 1(a)-(d), respectively. Fig. 1(a) indicates that the proposed AFTC scheme can force the output $\boldsymbol{q}$ of RM to track the desired trajectory $\boldsymbol{q}_d$ with satisfactory performance. It is seen from Fig. 1(b) that the the tracking errors $e_{1,1}$ and $e_{1,2}$ are bounded. Fig. 1(c) shows the curve of control input $\boldsymbol{\tau}$, which is bounded and reasonable, and the boundedness of the estimation $\hat{\theta}$ is seen in Fig. 1(d). These results demonstrate that all signals in the closed-loop tracking control system are bounded as proved Theorem 1.

To illuminate the superiority of the proposed AFTC scheme, a simulation comparison with the robust adaptive control (RAC) scheme proposed in [19] is carried out. In simulation, the design parameters can be caught in detail in [19] and the initial states $\boldsymbol{q}(\mathbf{0})$ and $\dot{\boldsymbol{q}}(0)$ are identical to the counterparts for the simulations under the FT control scheme.

The simulation results under the RAC scheme are plotted using dash line in Fig. 1(a)-(d), respectively. It is obvious from Fig.1(a)-(b) that the AFTC scheme exhibits superior control performance to the RAC scheme on the convergence rate and the control accuracy. From Fig. 1(c), the control efforts of two schemes are almost identical. Therefore, the simulation and comparison results demonstrate the desirable features of the proposed control scheme, such as FT

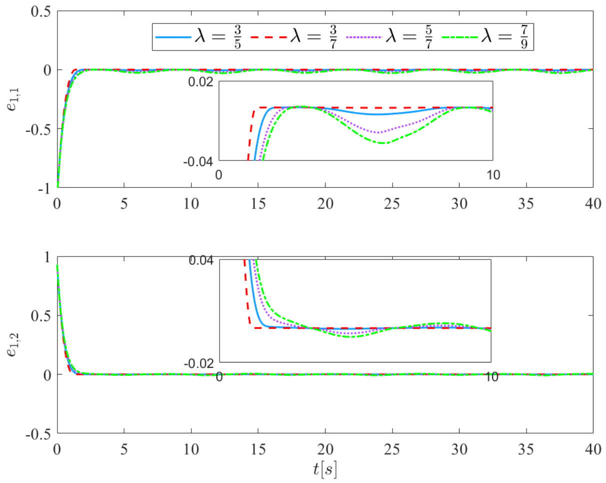

FIGURE 2. Comparison of control performance.

TABLE 1. Performance index comparison under different λ.

Index	Item	$\lambda=\frac{3}{5}$	$\lambda=\frac{3}{7}$	$\lambda=\frac{5}{7}$	$\lambda=\frac{7}{9}$
ST	$e_{1,1}$	1.38	1.11	1.59	1.72
	$e_{1,2}$	1.18	0.96	1.37	1.48
IAE	$e_{1,1}$	0.585	0.451	0.859	1.04
	$e_{1,2}$	0.391	0.344	0.471	0.537
	$S_{1,1}$	1.163	0.566	1.711	1.931
	$S_{1,2}$	0.289	0.093	0.475	0.557
MIAC	τ_1	3.688	3.678	3.688	3.688
	τ_2	1.2	1.2	1.2	1.2

convergence, and robustness against the disturbances and nonparametric uncertainties.

B. PERFORMANCE TEST

To analyze the impact of λ on the control performance, the simulation comparison with the different λ and same other design parameters is carried out. The simulation results on the tracking error $\boldsymbol{e}$ are shown in Fig. 2, and the quantitative evaluation results on the tracking error e and the variable S are listed in Table 1. In Table 1, ST denotes the settling time, IAE denotes the integrated absolute error and MIAC $= \frac{\int_{t_0}^{t_m} |\tau(t)|\, dt}{t_m - t_0}$ denotes the mean integrated absolute control, which are used to evaluate the transient and steady state performance, and energy consumption. From Fig. 2 and Table 1, it can be known that the smaller λ is, the better control accuracy and the fast convergence rate is. In addition, from the MIAC, λ has little impact on the control efforts. That is, the control performance can be improved by appropriately selecting λ.

Moreover, to illustrate the effectiveness of the initial value conditions $\boldsymbol{q}(0)$ and $\dot{\boldsymbol{q}}(0)$ on the control performance, simulations are carried out under four cases, and the initial conditions $\boldsymbol{q}(0)$ and $\dot{\boldsymbol{q}}(0)$ are listed in Table 2. The simulation results are shown in Fig. 3(a)-(b), and the performance indices are summarized in Table 3. From Fig. 3(a) and Table 3, it can be found that the control accuracy is not effected by

TABLE 2. Initial condition.

Item	C_1	C_2	C_3	C_4
$\boldsymbol{q}(0)$	$[-2.0; 2.5]$	$[-1.5; 3.0]$	$[-1.5; 2.5]$	$[-2.0; 3.0]$
$\dot{\boldsymbol{q}}(0)$	$[0; 0]$	$[0; 0]$	$[0.2; 0.1]$	$[0.2; 0.1]$

TABLE 3. Performance index comparison under different $q(0)$ and $\dot{q}(0)$.

Index	Item	C_1	C_2	C_3	C_4
IAE	$e_{1,1}$	0.7814	1.046	0.804	1.046
	$e_{1,2}$	0.648	0.929	0.653	0.931
MIAC	τ_1	3.678	3.678	4.75	4.73
	τ_2	1.203	1.206	1.555	1.557

the initial value of $\dot{\boldsymbol{q}}(0)$. However, the initial values of $\boldsymbol{q}(0)$ directly affect the convergence time, which is consistent with the characteristics of a finite time control system. Moreover, it can be clearly seen from Fig. 3(b) and Table 3 that the energy consumption is not affected by $\boldsymbol{q}(0)$, but affected by $\dot{\boldsymbol{q}}(0)$. Besides, from Fig.7, the larger the initial value of $\boldsymbol{q}(0)$, the more saturated the actuator, because the term $\varrho(\boldsymbol{S})$ in (22) depends on the initial value of $\boldsymbol{q}(0)$. We also find from Figs. 3(a)-(b) and Table 3 that the initial conditions $\boldsymbol{q}(0)$ and $\dot{\boldsymbol{q}}(0)$ do not affect the steady-state performance, which indicates that the proposed control scheme guarantees the satisfying control performance of uncertain ELSs under various initial conditions $\boldsymbol{q}(0)$ and $\dot{\boldsymbol{q}}(0)$.

C. ROBUSTNESS TEST

In this subsection, we test the robustness of the proposed control scheme. In this context, two scenarios are taken into account in the simulation. In case 1, the model parameter perturbation is taken in account, i.e., $\Delta\boldsymbol{M}(\boldsymbol{q}) = 30\%\boldsymbol{M}(\boldsymbol{q})$, $\Delta\boldsymbol{C}(\boldsymbol{q},\dot{\boldsymbol{q}}) = 30\%\boldsymbol{C}(\boldsymbol{q},\dot{\boldsymbol{q}})$, $\Delta\boldsymbol{G}(\boldsymbol{q}) = 30\%\boldsymbol{G}(\boldsymbol{q})$ and $\Delta\boldsymbol{F}(\boldsymbol{q},\dot{\boldsymbol{q}}) = 30\%\boldsymbol{F}(\boldsymbol{q},\dot{\boldsymbol{q}})$. In case 2, not only the model parameter perturbation is considered, but also the stronger disturbance is taken into account, i.e., the disturbance is taken as $\boldsymbol{d} + \boldsymbol{\varpi}$, where $\dot{\boldsymbol{\varpi}} = -\boldsymbol{\Xi}^{-1}\boldsymbol{\varpi} + \boldsymbol{\Pi}\boldsymbol{\eta}$ with $\boldsymbol{\Xi} = diag[1, 1]$ and $\boldsymbol{\Pi} = diag[1.5, 1]$, and $\boldsymbol{\eta}$ being a vector of zero-mean Gaussian white noises. In addition, the design parameters and initial conditions are taken the same as that of subsection A.

The simulation results and performance indices are presented in Fig.4(a)-(b) and Table 4, respectively, from which we can find that the control accuracy is almost the same under the different levels of disturbance. Moreover, from Tables 2 and 4, it can be clearly seen that our proposed control scheme can still ensure satisfactory control performance even if there exists the model parameter perturbation in the closed-loop control systems of ELSs. Therefore, the simulation results show that the proposed control scheme is of the robustness performance against to uncertainties including nonparametric uncertainties and unknown disturbances.

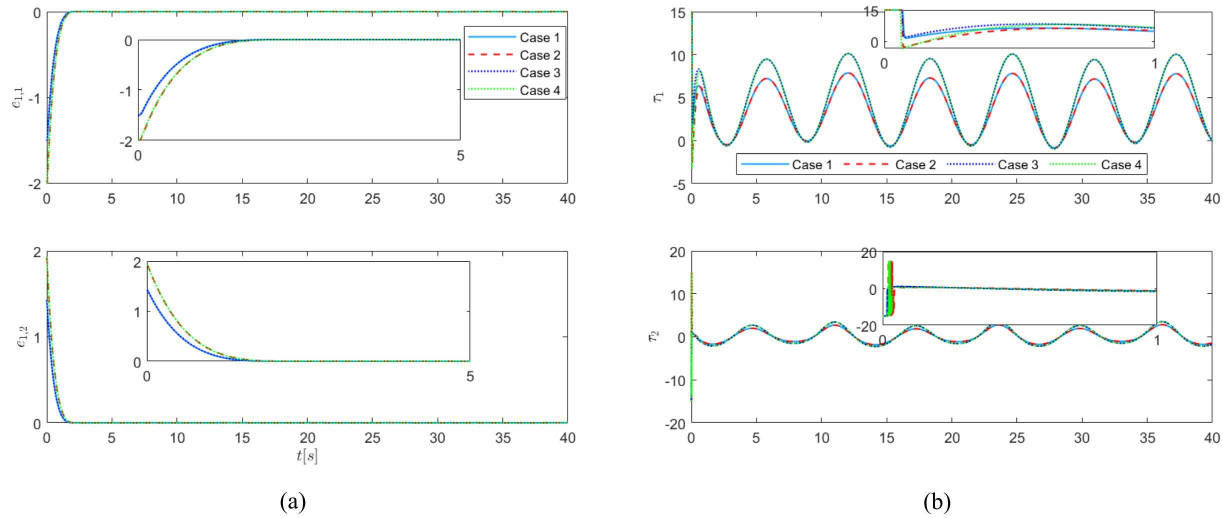

FIGURE 3. Simulation results under four cases. (a) Tracking error e_1. (b) Control input τ.

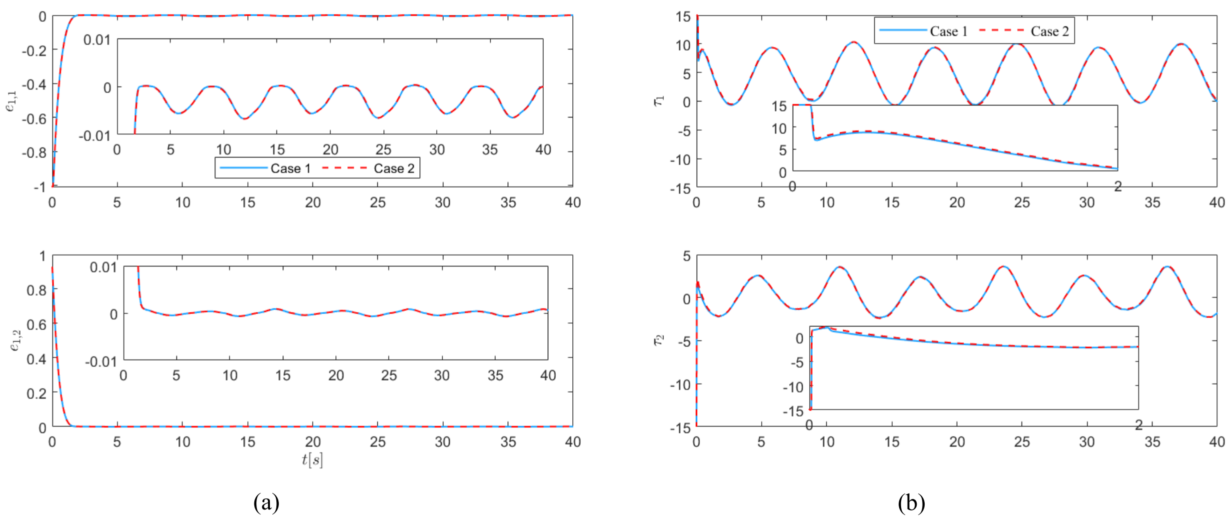

FIGURE 4. Simulation results in cases 1-2. (a) Tracking error e_1. (b) Control input τ.

TABLE 4. Performance index comparison in two scenarios.

Index	Item	Case 1	Case 2
IAE	$e_{1,1}$	0.653	0.653
	$e_{1,2}$	0.392	0.392
MIAC	τ_1	4.795	4.777
	τ_2	1.558	1.555

V. CONCLUSION

In this paper, a novel robust adaptive tracking control scheme has been developed for the ELSs subject to nonparametric uncertainties, unknown disturbances and input saturation. Under the developed control scheme, the trajectories of ELSs converge to a small region around the equilibrium point in finite time. In the control design, the lumped uncertain term caused by uncertain model parameters and external disturbances is formulated by a linear parametric form with a single parameter utilizing the LIP structure of the upper bound of uncertainties. As a result, any *prior* knowledge on the uncertainties is not required and the designed control law is not dependent of the nature of the uncertainties. Note that the settling time function in the developed FT control scheme is dependent on the system initial conditions, which would be a limitation in practical application. In the future, the work is to develop a control scheme which does not depend on the initial conditions of the systems.

REFERENCES

[1] R. Ortega and M. W. Spong, "Adaptive motion control of rigid robots: A tutorial," *Automatica*, vol. 25, no. 6, pp. 877–888, Nov. 1989.

[2] G. Zhu and J. Du, "Robust adaptive neural practical fixed-time tracking control for uncertain euler-Lagrange systems under input saturations," *Neurocomputing*, vol. 412, pp. 502–513, Oct. 2020.

[3] I. Tanyer, E. Tatlicioglu, and E. Zergeroglu, "Model reference tracking control of an aircraft: A robust adaptive approach," *Int. J. Syst. Sci.*, vol. 48, no. 7, pp. 1428–1437, May 2017.

[4] G. Zhu and J. Du, "Global robust adaptive trajectory tracking control for surface ships under input saturation," *IEEE J. Ocean. Eng.*, vol. 45, no. 2, pp. 442–450, Apr. 2020.

[5] H. Yu, C. Guo, and Z. Yan, "Globally finite-time stable three-dimensional trajectory-tracking control of underactuated UUVs," *Ocean Eng.*, vol. 189, Oct. 2019, Art. no. 106329, doi: 10.1016/j.oceaneng.2019.106329.

[6] E. Tatlicioglu, N. Cobanoglu, and E. Zergeroglu, "Neural network-based repetitive learning control of Euler Lagrange systems: An output feedback approach," *IEEE Control Syst. Lett.*, vol. 2, no. 1, pp. 13–18, Jan. 2018.

[7] S. Zhang, Y. Dong, Y. Ouyang, Z. Yin, and K. Peng, "Adaptive neural control for robotic manipulators with output constraints and uncertainties," *IEEE Trans. Neural Netw. Learn. Syst.*, vol. 29, no. 11, pp. 5554–5564, Nov. 2018.

[8] Z.-M. Li and J. H. Park, "Dissipative fuzzy tracking control for nonlinear networked systems with quantization," *IEEE Trans. Syst., Man, Cybern. Syst.*, early access, Sep. 12, 2018, doi: 10.1109/TSMC.2018.2866996.

[9] N. Sadegh and R. Horowitz, "An exponentially stable adaptive control law for robot manipulators," *IEEE Trans. Robot. Autom.*, vol. 6, no. 4, pp. 491–496, Aug. 1990.

[10] P. M. Patre, W. Mackunis, C. Makkar, C. Makkar, W. E. Dixon, "Asymptotic tracking for systems with structured and unstructured uncertainties," *IEEE Trans. Control Syst. Techn.*, vol. 16, no. 2, pp. 373–379, Mar. 2008.

[11] R. Hayat, M. Leibold, and M. Buss, "Robust-adaptive controller design for robot manipulators using the $\mathcal{H}_\infty$ approach," *IEEE Access*, vol. 6, pp. 51626–51639, 2018.

[12] H. G. Sage, M. F. De Mathelin, and E. Ostertag, "Robust control of robot manipulators: A survey," *Int. J. Control*, vol. 72, no. 16, pp. 1498–1522, Jan. 1999.

[13] L. Bascetta and P. Rocco, "Revising the robust-control design for rigid robot manipulators," *IEEE Trans. Robot.*, vol. 26, no. 1, pp. 180–187, Feb. 2010.

[14] J. J. Slotine and S. S. Sastry, "Tracking control of non-Linear systems using sliding surfaces, with application to robot manipulators," *Int. J. Control.*, vol. 38, no. 2, pp. 465–492, Jun. 1983.

[15] F. Garelli, L. Gracia, A. Sala, and P. Albertos, "Sliding mode speed auto-regulation technique for robotic tracking," *Robot. Auto. Syst.*, vol. 59, nos. 7–8, pp. 519–529, Jul. 2011.

[16] X. Liu, H. Su, B. Yao, and J. Chu, "Adaptive robust control of a class of uncertain nonlinear systems with unknown sinusoidal disturbances," in *Proc. 47th IEEE Conf. Decis. Control*, 2008, pp. 2594–2599.

[17] A. Papadimitropoulos, G. A. Rovithakis, and T. Parisini, "Fault detection in mechanical systems with friction phenomena: An online neural approximation approach," *IEEE Trans. Neural Netw.*, vol. 18, no. 4, pp. 1067–1082, Jul. 2007.

[18] H. Lee and V. I. Utkin, "Chattering suppression methods in sliding mode control systems," *Annu. Rev. Control*, vol. 31, no. 2, pp. 179–188, Jan. 2007.

[19] S. Roy, S. B. Roy, and I. N. Kar, "Adaptive–robust control of Euler–Lagrange systems with linearly parametrizable uncertainty bound," *IEEE Trans. Control Syst. Technol.*, vol. 26, no. 5, pp. 1842–1850, Sep. 2018.

[20] S. Islam, P. X. Liu, and A. El Saddik, "Robust control of four-rotor unmanned aerial vehicle with disturbance uncertainty," *IEEE Trans. Ind. Electron.*, vol. 62, no. 3, pp. 1563–1571, Mar. 2015.

[21] J. Baek, M. Jin, and S. Han, "A new adaptive sliding-mode control scheme for application to robot manipulators," *IEEE Trans. Ind. Electron.*, vol. 63, no. 6, pp. 3628–3637, Jun. 2016.

[22] Z. Sun, G. Zhang, J. Yang, and W. Zhang, "Research on the sliding mode control for underactuated surface vessels via parameter estimation," *Nonlinear Dyn.*, vol. 91, no. 2, pp. 1163–1175, Jan. 2018.

[23] Z. Song and K. Sun, "Adaptive sliding mode tracking control for uncertain euler-Lagrange system," *IEEE Access*, vol. 7, pp. 56817–56825, 2019.

[24] C. Ren, N. Rong, S. He, "Finite-time positiveness and distributed control of Lipschitz nonlinear multi-agent systems," *J. Frankl. Inst.*, vol. 356, no. 15, pp. 8080–8092, Oct. 2019.

[25] C. Ren, S. He, X. Luan, F. Liu, and H. R. Karimi, "Finite-time L_2-gain asynchronous control for continuous-time positive hidden Markov jump systemsvia T-S fuzzy model approach," *IEEE Trans. Cybern.*, early access, Jan. 10, 2020, doi: 10.1109/TCYB.2020.2996743.

[26] Y. Hong, Y. Xu, and J. Huang, "Finite-time control for robot manipulators," *Syst. Control Lett.*, vol. 46, no. 4, pp. 243–253, Jul. 2002.

[27] Y. Su, "Global continuous finite-time tracking of robot manipulators," *Int. J. Robust Nonlinear Control*, vol. 19, no. 17, pp. 1871–1885, Nov. 2009.

[28] D. Zhao, F. Gao, S. Li, and Q. Zhu, "Robust finite-time control approach for robotic manipulators," *IET Control Theory Appl.*, vol. 4, no. 1, pp. 1–15, Jan. 2010.

[29] S. Yu, X. Yu, B. Shirinzadeh, and Z. Man, "Continuous finite-time control for robotic manipulators with terminal sliding mode," *Automatica*, vol. 41, no. 11, pp. 1957–1964, Nov. 2005.

[30] M. Galicki, "Finite-time trajectory tracking control in a task space of robotic manipulators," *Automatica*, vol. 67, pp. 165–170, May 2016.

[31] F. A. Miranda-Villatoro, B. Brogliato, and F. Castanos, "Multivalued robust tracking control of Lagrange systems: Continuous and discrete-time algorithms," *IEEE Trans. Autom. Control*, vol. 62, no. 9, pp. 4436–4450, Sep. 2017.

[32] S. Mondal and C. Mahanta, "Adaptive second order terminal sliding mode controller for robotic manipulators," *J. Franklin Inst.*, vol. 351, no. 4, pp. 2356–2377, Apr. 2014.

[33] L. Wang, T. Chai, and L. Zhai, "Neural-network-based terminal sliding-mode control of robotic manipulators including actuator dynamics," *IEEE Trans. Ind. Electron.*, vol. 56, no. 9, pp. 3296–3304, Sep. 2009.

[34] Y. Yang, C. Hua, J. Li, and X. Guan, "Robust adaptive uniform exact tracking control for uncertain Euler–Lagrange system," *Int. J. Control*, vol. 90, no. 12, pp. 2711–2730, Dec. 2016.

[35] M. Boukattaya, N. Mezghani, and T. Damak, "Adaptive nonsingular fast terminal sliding-mode control for the tracking problem of uncertain dynamical systems," *ISA Trans.*, vol. 77, pp. 1–19, Jun. 2018.

[36] M.-D. Tran and H.-J. Kang, "A novel adaptive finite-time tracking control for robotic manipulators using nonsingular terminal sliding mode and RBF neural networks," *Int. J. Precis. Eng. Manuf.*, vol. 17, no. 7, pp. 863–870, Jul. 2016.

[37] Y. Mi, J. Yao, W. Deng, and Y. Xie, "Output feedback control of integrator systems with disturbance and input saturation," *J. Franklin Inst.*, vol. 357, no. 14, pp. 9330–9350, Sep. 2020.

[38] D. López-Araujo, A. Loría, and A. Zavala-Río, "Adaptive tracking control of Euler–Lagrange systems with bounded controls," *Int. J. Adapt. Control Signal Process.*, vol. 31, no. 3, pp. 299–313, Mar. 2017.

[39] E. Arefinia, H. A. Talebi, and A. Doustmohammadi, "A robust adaptive model reference impedance control of a robotic manipulator with actuator saturation," *IEEE Trans. Syst., Man, Cybern., Syst.*, vol. 50, no. 2, pp. 409–420, Feb. 2020.

[40] W. He, Y. Dong, and C. Sun, "Adaptive neural impedance control of a robotic manipulator with input saturation," *IEEE Trans. Syst., Man, Cybern., Syst.*, vol. 46, no. 3, pp. 334–344, Mar. 2016.

[41] Y. Su and J. Swevers, "Finite-time tracking control for robot manipulators with actuator saturation," *Robot. Comput.-Integr. Manuf.*, vol. 30, no. 2, pp. 91–98, Apr. 2014.

[42] H.-T. Chen, S.-M. Song, and Z.-B. Zhu, "Robust finite-time attitude tracking control of rigid spacecraft under actuator saturation," *Int. J. Control, Autom. Syst.*, vol. 16, no. 1, pp. 1–15, Mar. 2018.

[43] J. Ma, S. S. Ge, Z. Zheng, and D. Hu, "Adaptive NN control of a class of nonlinear systems with asymmetric saturation actuators," *IEEE Trans. Neural Netw. Learn. Syst.*, vol. 26, no. 7, pp. 1532–1538, Jul. 2015.

[44] C. Qian and W. Lin, "Non-lipschitz continuous stabilizers for nonlinear systems with uncontrollable unstable linearization," *Syst. Control Lett.*, vol. 42, no. 3, pp. 185–200, Mar. 2001.